Letter

Reduced-order Galerkin models of plane Couette flow

André V. G. Cavalieri [1,*] and Petrônio A. S. Nogueira [2,†]

[1]*Divisão de Engenharia Aeroespacial, Instituto Tecnológico de Aeronáutica, São José dos Campos, SP 12228-900, Brazil*
[2]*Department of Mechanical and Aerospace Engineering, Laboratory for Turbulence Research in Aerospace and Combustion, Monash University, Clayton VIC 3800, Australia*

Reduced-order models were derived for plane Couette flow using Galerkin projection, with orthonormal basis functions taken as the leading controllability modes of the linearized Navier-Stokes system for a few low wave numbers. Resulting Galerkin systems comprise ordinary differential equations, with a number of degrees of freedom ranging from 144 to 600, which may be integrated to large times without any indication of numerical instability. The reduced-order models so obtained are also found to match statistics of direct numerical simulations at Reynolds number 500 and 1200 with reasonable accuracy, despite a truncation of orders of magnitude in the degrees of freedom of the system. The present models offer thus an interesting compromise between simplicity and accuracy in a canonical wall-bounded flow, with relatively few modes representing coherent structures in the flow and their dominant dynamics.

The complexity of the Navier-Stokes equation has motivated the development of reduced-order models (ROMs) over the years. By reducing a full model to a simplified system, computational gains may be achieved, but, perhaps more importantly, one greatly simplifies the dynamics, allowing a closer inspection of the mechanisms at play [1,2]. ROMs are also important to derive flow control schemes [3], as obtaining control laws may become prohibitively expensive when dealing with the full system.

A widespread technique for model reduction is Galerkin projection, where partial differential equations are projected onto a reduced set of modes that form a basis of a subspace of interest [4]. This is also attractive as such modes may be related to coherent structures in flows [5]. When Galerkin projections are applied to three-dimensional spatial modes, one obtains a system of ordinary differential equations that models the time evolution of mode amplitude [2], and one may easily explore the interplay between coherent structures, or modes, by examining energy exchanges in the system [6,7]. In some cases, Fourier modes may be directly used in a Galerkin projection [1,8], but in more complex flows, with nonhomogeneous directions, Fourier modes may not be applicable. A common choice of modes is based on proper orthogonal decomposition (POD) of numerical or experimental databases. POD provides an orthonormal basis that is optimal in representing the energy of the database at hand, and, for that property, was chosen in the derivation of a few ROMs in the literature [2,9–11].

Unlike Galerkin models built with analytical basis functions [1,7,12,13], it is often mentioned that numerical Galerkin systems built using POD require a closure model to represent neglected

———————
*andre@ita.br
†petronio.nogueira@monash.edu

modes, as discussed by Grimberg *et al.* [14] and Callaham *et al.* [15]; otherwise, one may obtain numerically unstable ROMs. Such closure models were developed in the early work of Aubry *et al.* [9], and modeling works have attempted various forms of closure in order to obtain a numerically stable and accurate Galerkin system [10,11,15]; a comprehensive review is provided by Ahmed *et al.* [16]. In this work, we derive numerical Galerkin models for Couette flow with arbitrary order, which will be shown to be numerically stable and reproduce standard turbulence statistics with reasonable accuracy. This raises questions on the actual need of closure models to stabilize Galerkin models. Plane Couette flow is an ideal case for such a study, as a canonical flow for studies of transition and of wall-bounded turbulence. Successful model reductions of the Navier-Stokes system have already been obtained, either by a Galerkin projection along a spatial direction [17], or by restricting the possible nonlinear interactions in the system [18]. Moreover, it is known that this flow is dominated by coherent structures spanning the entire space between walls [19–21], which may be modeled using the linearized Navier-Stokes system [22–25]; such a feature enables the description of the flow with a low or moderate number of modes representing coherent structures.

Following the same conventions in [7], we consider incompressible plane Couette flow in Cartesian coordinates (x, y, z) corresponding to streamwise, wall-normal, and spanwise directions, with a zero pressure gradient along x. Quantities are normalized by wall velocity and half-wall separation, such that the walls are placed at $y = \pm 1$ and move with velocity $u = \pm 1$. The velocity vector $\mathbf{u}$, taken as fluctuations around the laminar solution $\mathbf{u}_0 = [y \quad 0 \quad 0]^T$, has components u, v, and w along each Cartesian coordinate. We consider a computational domain with periodic boundary conditions in x and z, with lengths given by L_x and L_z, respectively. Nonslip boundary conditions are imposed on the walls at $y = \pm 1$.

Galerkin models are obtained based on an inner product defined as

$$\langle \mathbf{f}, \mathbf{g} \rangle = \frac{1}{2L_x L_z} \int_0^{L_z} \int_{-1}^1 \int_0^{L_x} \mathbf{f}(x, y, z) \cdot \mathbf{g}(x, y, z) dx dy dz, \tag{1}$$

which for velocity fields in incompressible flows corresponds to the volume-averaged kinetic energy.

We consider a modal decomposition of the velocity fluctuations $\mathbf{u}$ around the laminar solution $\mathbf{u}_0 = [y \quad 0 \quad 0]^T$ as

$$\mathbf{u}(x, y, z, t) = \sum_j a_j(t) \mathbf{v}_j(x, y, z), \tag{2}$$

where each of the spatial modes $\mathbf{v}_j(x, y, z)$ satisfies the continuity equation and the boundary conditions, forming an orthonormal basis. We consider the Navier-Stokes equation for fluctuations around the laminar solution,

$$\frac{\partial \mathbf{u}}{\partial t} + (\mathbf{u}_0 \cdot \nabla)\mathbf{u} + (\mathbf{u} \cdot \nabla)\mathbf{u}_0 + (\mathbf{u} \cdot \nabla)\mathbf{u} = -\nabla p + \frac{1}{\mathrm{Re}} \nabla^2 \mathbf{u}, \tag{3}$$

where p is the pressure. Inserting the decomposition of Eqs. (2) in (3), and taking an inner product with $\mathbf{u}_i$, leads to a system of ordinary differential equations given by

$$\frac{da_i}{dt} = \frac{1}{\mathrm{Re}} \sum_j L_{i,j} a_j + \sum_j \tilde{L}_{i,j} a_j + \sum_j \sum_k Q_{i,j,k} a_j a_k, \tag{4}$$

where

$$L_{i,j} = \langle \nabla^2 \mathbf{v_j}, \mathbf{v_i} \rangle, \tag{5}$$

$$\tilde{L}_{i,j} = -\langle [(\mathbf{v_j} \cdot \nabla)\mathbf{u_0} + (\mathbf{u_0} \cdot \nabla)\mathbf{v_j}], \mathbf{v_i} \rangle, \tag{6}$$

$$Q_{i,j,k} = -\langle (\mathbf{v_j} \cdot \nabla)\mathbf{v_k}, \mathbf{v_i} \rangle. \tag{7}$$

TABLE I. Galerkin systems of this work.

N	k_x/α	$n_{\mathrm{modes},y}$	k_z/β
144	0, 1	16	−1, 0, 1
360	0, 1	24	−2, −1, 0, 1, 2
600	0, 1, 2	24	−2, −1, 0, 1, 2

The pressure is eliminated from the equations using the divergence-free property of the modes. The coefficients in the ODE system of Eq. (4) include two linear terms $L_{i,j}$ and $\tilde{L}_{i,j}$, corresponding, respectively, to the viscous term and to interaction with the laminar solution $\mathbf{u}_0$. The quadratic term $Q_{i,j,k}$ represents nonlinear interactions among modes.

Orthogonal modes $\mathbf{v}_i$ may be obtained as eigenfunctions of the controllability Gramian, considering the linearized Navier-Stokes system forced with white noise in space and time [26,27]. We follow the formulation of Jovanovic and Bamieh [27] and obtain orthonormal velocity modes considering as base flow the laminar solution for Couette flow, considering white-noise forcing in the momentum equations. This is done for combinations of streamwise and spanwise wave numbers k_x and k_z, as indicated in Table I. The supplemental material [28] shows results for Galerkin systems with other numbers of modes, all of which display behavior similar to the three ROMs studied here. A normal-mode ansatz for controllability modes implies a dependence $\mathbf{v}_i(x, y, z) = \hat{\mathbf{v}}_i(y)e^{i(k_x x + k_z z)}$, which leads to complex-valued modes; we deal here with real modes by taking separate modes for the real and imaginary parts of $\hat{\mathbf{v}}_i(y)e^{i(k_x x + k_z z)}$, which leads to a pair of modes that only differ by a phase shift of $\pi/2$. The wave numbers k_x and k_z are taken as integer multiples of the fundamental wave numbers $\alpha = 2\pi/L_x$ and $\beta = 2\pi/L_z$, respectively, in order to match the periodicity imposed by the domain dimensions L_x and L_z. Since modes with $(-k_x, -k_z)$ are simply complex conjugates of (k_x, k_z), only positive k_x is considered; for $k_x = 0$, only $k_z \geqslant 0$ needs to be included in the basis. For $k_x = k_z = 0$, corresponding to mean-flow modes, the linearized operator becomes singular and we need to resort to a different option. In this case, we have taken Stokes modes, eigenfunctions of viscous diffusion, as in earlier works [1]. The number of controllability modes in Table I was chosen to ensure the stability of the laminar solution of Couette flow; stronger truncations were seen to lead to an unstable laminar solution, which would not be physical.

The choice of controllability modes is similar to the use of POD to derive several reduced-order models in the literature [2,9,11], as controllability modes correspond to POD for the linear system driven with white noise [26,27,29,30]. The leading modes represent streaks and rolls, which are dominant coherent structures in Couette flow, and also for other wall-bounded turbulent flows [31,32]; some sample modes are shown and discussed in the supplemental material [28]. The advantage of using controllability modes is that one does not need a full numerical or experimental database to obtain POD modes; here, the linearized operator is used to obtain an orthonormal basis that approximates large-scale structures in the flow. Unless otherwise specified, for the present ROMs we have constructed bases with controllability modes taken at a low Reynolds number, Re = 100. Values of Reynolds number matching the cases explored here, Re = 500 and 1200, were also attempted, but led to slightly worse quantitative agreement with reference statistics; we will later illustrate some results for a basis constructed using Re = 500. Controllability modes for higher Re become increasingly localized in space or oscillatory, which contrasts with observations of coherent structures for Couette flow [19–21]. The better performance of a basis constructed at low Re may be a further indication that linearized models obtained considering additional viscous effects, akin to an eddy viscosity, may be a better representation of coherent structures in turbulent flows, as explored in recent works [33,34]. It is nonetheless interesting to use a fixed set of modes for various Reynolds numbers, as it allows us to use a single ROM for several Re, such that invariant solutions and bifurcations may be studied with ease [13,35].
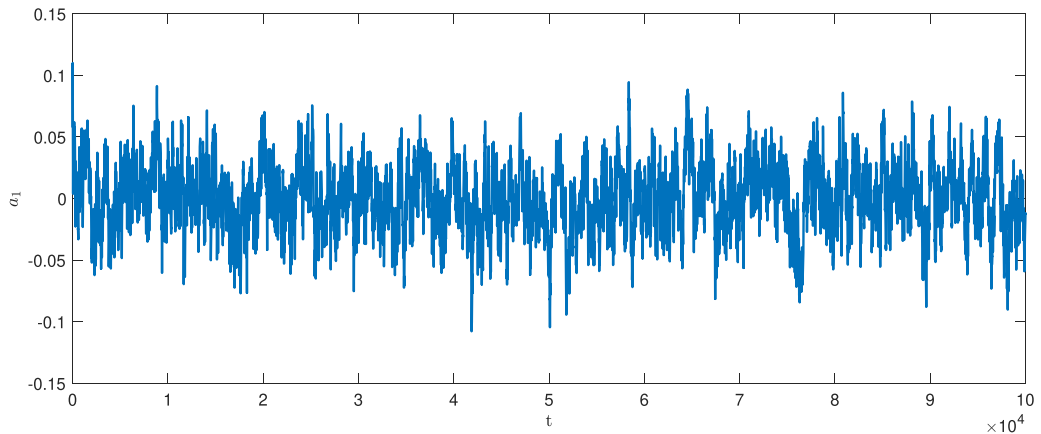
FIG. 1. Time series of the first mode coefficient, $a_1(t)$, from an integration of the $N = 144$ ROM at Re = 1200.

The controllability modes are obtained using spectral methods, with a Chebyshev discretization in y following Weideman and Reddy [36], considering 65 Chebyshev polynomials for all cases, consistently with discretizations used in DNS. The direct and adjoint linearized operators are written in matrix form, and the resulting Lyapunov equation (which, in matrix form, becomes a Sylvester equation) is solved numerically using the LAPACK routine *ztrsyl* in its MATLAB implementation. The modes so obtained were verified to satisfy the continuity equation to machine precision. Quadratures were carried out using Clenshaw-Curtis quadrature in y [37], and the standard trapezoidal rule in x and z as it has spectral accuracy for a Fourier discretization [38]. The domain considered here has lengths $(L_x, L_z) = (2\pi, \pi)$, a domain size often used in studies of transitional Couette flow [39], discretized with 16 points in x and z and 65 points in y; the lower number of points in x and z is nonetheless well beyond the required amount for dealiasing the few Fourier modes at hand. Time integration is carried out with a standard 4th/5th Runge-Kutta method for 3000 nondimensional time units in order to collect statistics. A random initial condition was taken, and statistics are collected after a transient of 500 time units. Albeit not shown here, the models display transient chaos, as in our earlier work [7], but with longer lifetimes, well beyond the 3000 time units considered for statistics. The models have been shown to be numerically stable, with integrations carried out to much higher times, up to 10^6, which is much longer than typical direct numerical simulations of turbulent Couette flow. A sample time series in shown in Fig. 1, with integration carried out for 10^5 time units without any sign of numerical instability, such as reported in the literature to occur in about 100 nondimensional time units [14].

The statistics obtained with the Galerkin systems of Table I are shown in Fig. 2 for Re = 500. We show the mean velocity profile U, which results from the $k_x = k_z = 0$ modes in the ROM, and the root-mean-square (RMS) values of the three velocity components u, v, and w. Results are compared to reference DNS statistics obtained with Channelflow [40], with a grid resolution of $(N_x, N_y, N_z) = (32, 65, 32)$, times a 3/2 factor in N_x and N_z for dealiasing; the DNS thus has a number of degrees of freedom (DoFs) of about 10^5. We initially focus on the results obtained with Re = 100 controllability modes, displayed in full colored lines. The various ROMs display a reasonable agreement with the DNS statistics, with a somewhat lower accuracy for the strongest truncation with $N = 144$ DoFs. The present reductions of two to three orders of magnitude retain nonetheless the salient features of turbulent Couette flow. For the truncations at hand, which are coarse approximations of the full system, we are still far from a monotonic convergence to DNS. Such a nonmonotonic convergence was observed for turbulent channel flow solved with coarse numerical resolutions [41,42]. One would thus expect monotonic convergence to reference statistics
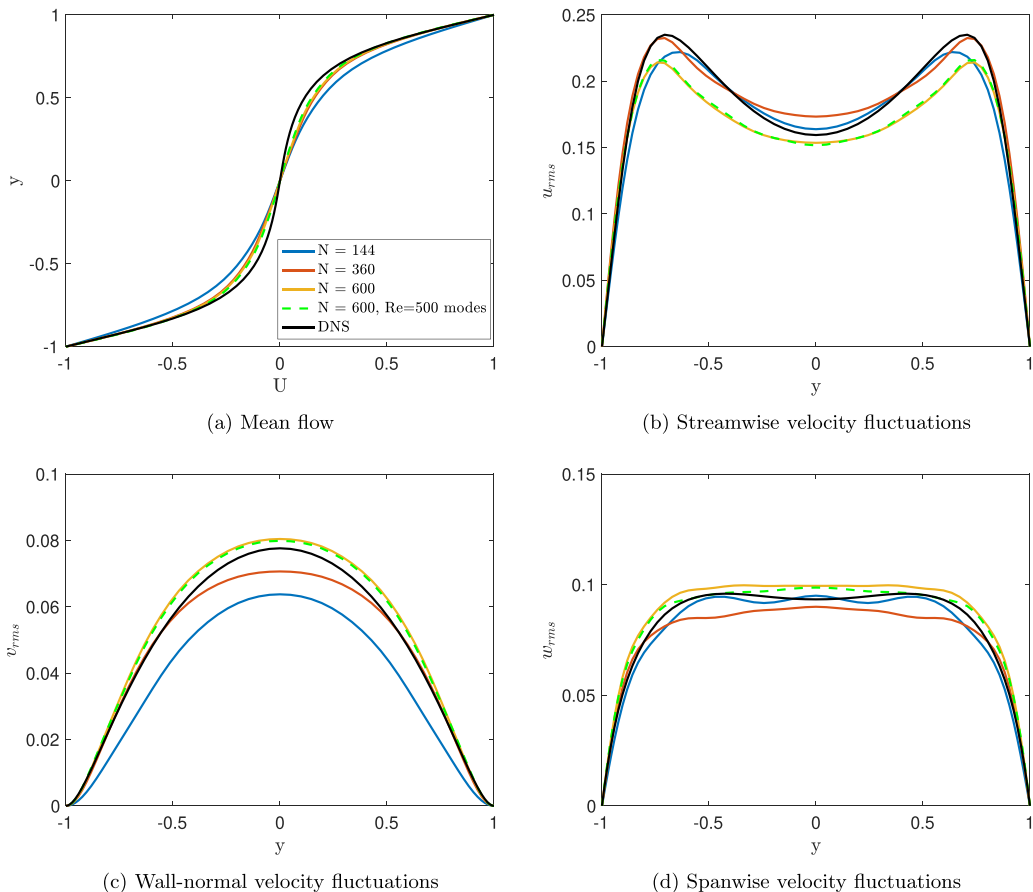
(a) Mean flow

(b) Streamwise velocity fluctuations

(c) Wall-normal velocity fluctuations

(d) Spanwise velocity fluctuations

FIG. 2. Statistics of ROMs and DNS for Re = 500. Full colored lines show results obtained with Re = 100 controllability modes; green dashed line for Re = 500 controllability modes.

only for a number of DoFs significantly higher than the present models; however, it is encouraging that all present discretizations lead to statistics in fair agreement with DNS data. The present ROM displays an agreement to reference DNS results that is equal to or better than earlier POD-Galerkin ROMs for plane Couette flow [10,11], which use DNS data to calibrate closure models. Here, no calibration is performed, and accurate dynamics are obtained by simply increasing the number of modes in the basis. The agreement in statistics is also equal to or better than what is obtained when some nonlinear interactions in the Navier-Stokes system are neglected [43].

The model results are compared to DNS for Re = 1200 in Fig. 3. In this case, the DNS was carried out with $(N_x, N_y, N_z) = (64, 65, 64)$ to maintain typical resolutions of direct numerical simulation, leading to a number of DoFs of about 5×10^5. The present ROMs thus have a reduction of three to four orders of magnitude in the number of DoFs, and they maintain nonetheless a reasonable quantitative agreement with reference statistics. The profiles in y display oscillations in some of the cases, which we attribute to a low number of controllability modes to discretize the y direction. This is observed for the w statistics of the $N = 144$ ROM for Re = 500, and for the three ROMs as Re is increased to 1200 in Fig. 3.

The green dashed lines in Figs. 2 and 3 show statistics of the largest ROM, constructed with controllability modes taken at Re = 500. For the "design" Re = 500, this ROM has almost the same velocity statistics as the one constructed with Re = 100 controllability modes. This is reassuring, as

(a) Mean flow

(b) Streamwise velocity fluctuations

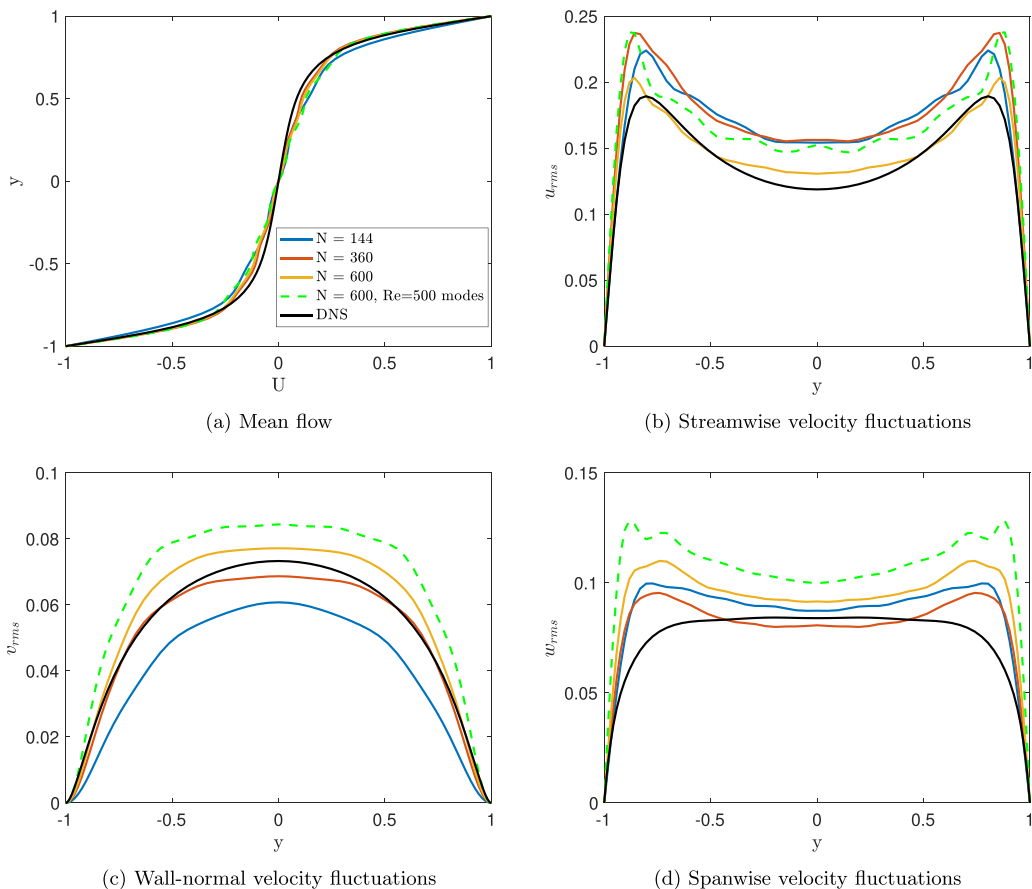(c) Wall-normal velocity fluctuations

(d) Spanwise velocity fluctuations

FIG. 3. Statistics of ROMs and DNS for Re = 1200. See the caption of Fig. 2.

it shows that the performance of the present models does not depend crucially on a specific choice of basis functions. However, when the basis is "off-design" at Re = 1200 the model statistics are further from the reference results. All ROMs tested are nonetheless stable and lead to reasonable statistics, but we observe that the convergence to DNS results depends on the choice of basis functions. In what follows, we will restrict ourselves to the ROMs constructed with Re = 100 controllability modes.

A further check of the accuracy of the ROMs was made by projecting the DNS data onto the modal basis $\mathbf{v}_i$ as

$$a_i^{(\mathrm{DNS})}(t) = \langle \mathbf{u}_{\mathrm{DNS}}, \mathbf{v}_i \rangle, \tag{8}$$

and then computing the RMS values of time coefficients a_i, obtained either from the ROM or from the projection of DNS data onto the modal basis following Eq. (8). Results are shown in Fig. 4 for the largest ROM with $N = 600$. The results for both Reynolds numbers show RMS values of modes decaying with increasing mode number, as expected as one goes from larger to smaller structures in a cascade. Focusing on the results for Re = 500, we observe similar trends between ROM results and DNS projections, which indicates that the ROM accurately represents the dynamics of Couette flow in the subspace spanned by the modal basis. However, the RMS values in the ROM are generally higher than the DNS projections, which may be understood by the lower number of DoFs in the ROM. In the DNS the energy may be transferred to smaller structures in higher wave numbers,
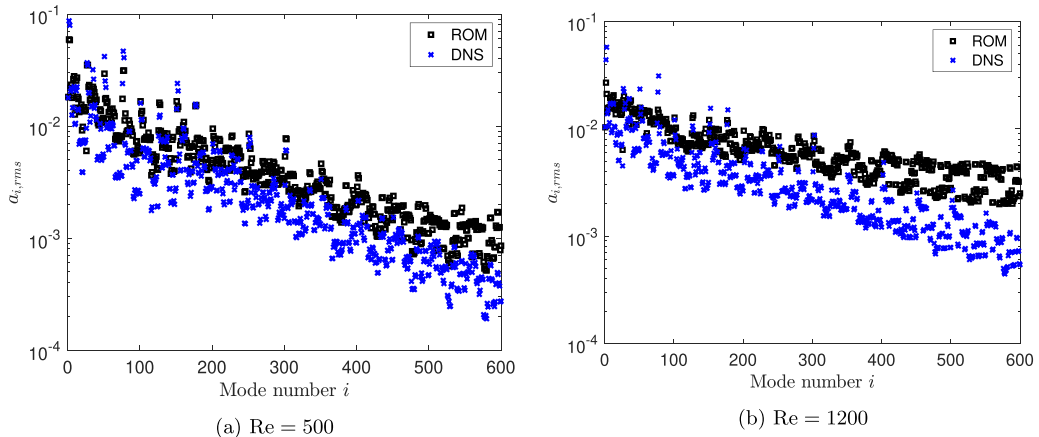
FIG. 4. Root-mean-square values of temporal coefficients $a_i(t)$ obtained either from a ROM simulation or from projection of DNS data onto the ROM modal basis. Results for the $N = 600$ ROM.

a process that is halted in the ROM as one truncates the basis, a phenomenon known as spectral blocking [44]. This is more visible in the Re = 1200 results, where RMS values of the ROM are significantly higher than the DNS projections, especially for higher-order modes, which is a symptom of accumulation of energy at higher modes due to their inability to transfer such energy to even smaller structures.

In summary, the ROMs obtained in this work, with a few hundred degrees of freedom, have been shown to represent the statistics and dynamics of plane Couette flow with moderate Reynolds number. The various truncations explored here all led to Galerkin systems which may be integrated in time without numerical instabilities, with model results that are reasonably close to reference DNS data despite the strong truncations. This indicates that inclusion of closure models [15,16] is not an essential feature of Galerkin models that are robust and accurate, at least for the flow configuration at hand, Reynolds number, choice of modes, and selected truncations. No numerical instability was observed in any of the present models, and a possible reason for this was the use of the same numerics of DNS in each step in the derivation of the ROM: the same pseudospectral methods of the DNS were used to compute derivatives and integrals. The robustness of the present model is similar to other Galerkin models built with analytical basis functions, which could be extensively integrated to large times without reported numerical issues [7,12,45]. However, inclusion of closure models may be beneficial for model accuracy, similarly to the use of subgrid models in large-eddy simulations, especially if one wishes to model high-Reynolds number flows with small dissipative lengthscales, which may require a large number of modes. The use of plane Couette flow, with its simple geometry and nonetheless complex dynamics, plenty of available literature on transition and turbulence, and the availability of open-source codes for direct numerical simulation, is suggested as a benchmark case for further development of reduced-order models.

The present ROMs open a number of interesting directions for further work on turbulence dynamics. It is straightforward to include or remove modes of interest, or even specific nonlinear interactions, and inspect the effect on the dynamics, as was done in our previous work [7]. This may help to probe further wall-bounded turbulence in search of nonlinear interactions with a dominant effect on dynamics. The observation that all ROMs in this work reproduce, within some error tolerance, the expected statistics of turbulent Couette flow indicates that the bulk of the dynamics may be described by nonlinear interaction involving a few modes representing coherent structures. Nonlinear interactions involving streamwise wave numbers have successfully been truncated in recent works [18,46,47], and the present ROMs also involve truncations in wall-normal and spanwise directions, retaining nonetheless a good amount of the underlying dynamics. Our ongoing

work on turbulent channel flow has also led to stable ROMs with similar accuracy, showing that the present observations are not specific to Couette flow. It is of course clear that in order to obtain DNS-type agreement with reference quantities, one needs DNS-range numbers of degrees of freedom, but significantly reduced systems may nonetheless provide an interesting compromise between simplicity and fidelity.

---

[1] F. Waleffe, On a self-sustaining process in shear flows, Phys. Fluids **9**, 883 (1997).

[2] B. R. Noack, K. Afanasiev, M. Morzynski, G. Tadmor, and F. Thiele, A hierarchy of low-dimensional models for the transient and post-transient cylinder wake, J. Fluid Mech. **497**, 335 (2003).

[3] A. Barbagalo, D. Sipp, and P. J. Schmid, Closed-loop control of an open cavity flow using reduced-order models, J. Fluid Mech. **641**, 1 (2009).

[4] C. W. Rowley and S. T. Dawson, Model reduction for flow analysis and control, Annu. Rev. Fluid Mech. **49**, 387 (2017).

[5] K. Taira, S. L. Brunton, S. T. Dawson, C. W. Rowley, T. Colonius, B. J. McKeon, O. T. Schmidt, S. Gordeyev, V. Theofilis, and L. S. Ukeiley, Modal analysis of fluid flows: An overview, AIAA J. **55** 4013 (2017).

[6] B. R. Noack, P. Papas, and P. A. Monkewitz, The need for a pressure-term representation in empirical galerkin models of incompressible shear flows, J. Fluid Mech. **523**, 339 (2005).

[7] A. V. G. Cavalieri, Structure interactions in a reduced-order model for wall-bounded turbulence, Phys. Rev. Fluids **6**, 034610 (2021).

[8] B. Saltzman, Finite amplitude free convection as an initial value problem—i, J. Atmos. Sci. **19**, 329 (1962).

[9] N. Aubry, P. Holmes, J. Lumley, and E. Stone, The dynamics of coherent structures in the wall region of a turbulent boundary layer, J. Fluid Mech. **192**, 115 (1988).

[10] T. Smith, J. Moehlis, and P. Holmes, Low-dimensional models for turbulent plane couette flow in a minimal flow unit, J. Fluid Mech. **538**, 71 (2005).

[11] Z. C. Khoo, C. H. Chan, and Y. Hwang, A sparse optimal closure for a reduced-order model of wall-bounded turbulence, J. Fluid Mech. **939**, A11 (2022).

[12] J. Moehlis, H. Faisst, and B. Eckhardt, A low-dimensional model for turbulent shear flows, New J. Phys. **6**, 56 (2004).

[13] A. V. G. Cavalieri, E. L. Rempel, and P. A. S. Nogueira, Transition to chaos in a reduced-order model of a shear layer, J. Fluid Mech. **932**, A43 (2022).

[14] S. Grimberg, C. Farhat, and N. Youkilis, On the stability of projection-based model order reduction for convection-dominated laminar and turbulent flows, J. Comput. Phys. **419**, 109681 (2020).

[15] J. L. Callaham, S. L. Brunton, and J.-C. Loiseau, On the role of nonlinear correlations in reduced-order modelling, J. Fluid Mech. **938**, A1 (2022).

[16] S. E. Ahmed, S. Pawar, O. San, A. Rasheed, T. Iliescu, and B. R. Noack, On closures for reduced order models—a spectrum of first-principle to machine-learned avenues, Phys. Fluids **33**, 091301 (2021).

[17] M. Lagha and P. Manneville, Modeling transitional plane Couette flow, Eur. Phys. J. B **58**, 433 (2007).

[18] V. L. Thomas, B. F. Farrell, P. J. Ioannou, and D. F. Gayme, A minimal model of self-sustaining turbulence, Phys. Fluids **27**, 105104 (2015).

[19] J. M. Hamilton, J. Kim, and F. Waleffe, Regeneration mechanisms of near-wall turbulence structures, J. Fluid Mech. **287**, 317 (1995).

[20] N. Tillmark and P. H. Alfredsson, Large scale structures in turbulent plane Couette flow, in *Advances in Turbulence VII* (Springer, Dordrecht, 1998), pp. 59–62.

[21] O. Kitoh and M. Umeki, Experimental study on large-scale streak structure in the core region of turbulent plane couette flow, Phys. Fluids **20**, 025107 (2008).

[22] P. J. Schmid and D. S. Henningson, *Stability and Transition in Shear Flows* (Springer, New York, 2001), Vol. 142.

[23] Y. Hwang and C. Cossu, Amplification of coherent streaks in the turbulent couette flow: an input–output analysis at low reynolds number, J. Fluid Mech. **643**, 333 (2010).

[24] L. Brandt, The lift-up effect: the linear mechanism behind transition and turbulence in shear flows, Eur. J. Mech. B Fluids **47**, 80 (2014).

[25] S. J. Illingworth, Streamwise-constant large-scale structures in couette and poiseuille flows, J. Fluid Mech. **889**, A13 (2020).

[26] B. F. Farrell and P. J. Ioannou, Stochastic forcing of the linearized navier–stokes equations, Phys. Fluids A **5**, 2600 (1993).

[27] M. R. Jovanović and B. Bamieh, Componentwise energy amplification in channel flows, J. Fluid Mech. **534**, 145 (2005).

[28] See Supplemental Material at http://link.aps.org/supplemental/10.1103/PhysRevFluids.7.L102601 for further information on controllability modes used to build the models, and for comparison of other ROMs, with various truncation levels, with reference DNS data.

[29] M. Ilak and C. W. Rowley, Modeling of transitional channel flow using balanced proper orthogonal decomposition, Phys. Fluids **20**, 034103 (2008).

[30] S. Bagheri, D. Henningson, J. Hoepffner, and P. Schmid, Input-output analysis and control design applied to a linear model of spatially developing flows, Appl. Mech. Rev. **62**, 020803 (2009).

[31] L. H. Hellström, I. Marusic, and A. J. Smits, Self-similarity of the large-scale motions in turbulent pipe flow, J. Fluid Mech. **792**, R1 (2016).

[32] L. I. Abreu, A. V. Cavalieri, P. Schlatter, R. Vinuesa, and D. S. Henningson, Spectral proper orthogonal decomposition and resolvent analysis of near-wall coherent structures in turbulent pipe flows, J. Fluid Mech. **900**, A11 (2020).

[33] P. Morra, O. Semeraro, D. S. Henningson, and C. Cossu, On the relevance of reynolds stresses in resolvent analyses of turbulent wall-bounded flows, J. Fluid Mech. **867**, 969 (2019).

[34] E. Pickering, G. Rigas, O. T. Schmidt, D. Sipp, and T. Colonius, Optimal eddy viscosity for resolvent-based models of coherent structures in turbulent jets, J. Fluid Mech. **917**, A29 (2021).

[35] J. Moehlis, H. Faisst, and B. Eckhardt, Periodic orbits and chaotic sets in a low-dimensional model for shear flows, SIAM J. Appl. Dyn. Syst. **4**, 352 (2005).

[36] J. A. Weideman and S. C. Reddy, A matlab differentiation matrix suite, ACM Trans. Math. Softw. **26**, 465 (2000).

[37] L. N. Trefethen, *Spectral Methods in MATLAB* (Society for Industrial Mathematics, 2000), Vol. 10.

[38] L. N. Trefethen and J. Weideman, The exponentially convergent trapezoidal rule, SIAM Rev. **56**, 385 (2014).

[39] T. Kreilos, B. Eckhardt, and T. M. Schneider, Increasing Lifetimes and the Growing Saddles of Shear Flow Turbulence, Phys. Rev. Lett. **112**, 044503 (2014).

[40] J. F. Gibson, F. Reetz, S. Azimi, A. Ferraro, T. Kreilos, H. Schrobsdorff, M. Farano, A. F. Yesil, S. S. Schütz, M. Culpo, and T. M. Schneider (unpublished).

[41] J. Meyers and P. Sagaut, Is plane-channel flow a friendly case for the testing of large-eddy simulation subgrid-scale models? Phys. Fluids **19**, 048105 (2007).

[42] A. Rasam, G. Brethouwer, P. Schlatter, Q. Li, and A. V. Johansson, Effects of modelling, resolution and anisotropy of subgrid-scales on large eddy simulations of channel flow, J. Turbul. **12**, N10 (2011).

[43] V. L. Thomas, B. K. Lieu, M. R. Jovanović, B. F. Farrell, P. J. Ioannou, and D. F. Gayme, Self-sustaining turbulence in a restricted nonlinear model of plane couette flow, Phys. Fluids **26**, 105112 (2014).

[44] J. P. Boyd, *Chebyshev and Fourier Spectral Methods* (Dover, Mineola, NY, 2001).

[45] M. Chantry, L. S. Tuckerman, and D. Barkley, Turbulent–laminar patterns in shear flows without walls, J. Fluid Mech. **791**, R8 (2016).

[46] J. Bretheim, C. Meneveau, and D. F. Gayme, Standard logarithmic mean velocity distribution in a band-limited restricted nonlinear model of turbulent flow in a half-channel, Phys. Fluids **27**, 011702 (2015).

[47] C. G. Hernández, Q. Yang, and Y. Hwang, Generalised quasilinear approximations of turbulent channel flow. part 1. streamwise nonlinear energy transfer, J. Fluid Mech. **936**, A33 (2022).